Astronomy
&
Astrophysics

The HARPS search for southern extrasolar planets[⋆,⋆⋆]

XXIII. 8 planetary companions to low-activity solar-type stars

D. Naef[1], M. Mayor[1], G. Lo Curto[2], F. Bouchy[3,4], C. Lovis[1], C. Moutou[5], W. Benz[6], F. Pepe[1], D. Queloz[1],
N.C. Santos[7], D. Ségransan[1], S. Udry[1], X. Bonfils[1,8], X. Delfosse[8], T. Forveille[8], G. Hébrard[3], C. Mordasini[6,9],
C. Perrier[8], I. Boisse[3], and D. Sosnowska[1]

[1] Observatoire Astronomique de l'Université de Genève, 51 Ch. des Maillettes, 1290 Sauverny, Switzerland
    e-mail: dominique.naef@unige.ch
[2] European Southern Observatory, Karl Schwarzschild Strasse 2, 85748 Garching bei München, Germany
[3] Institut d'Astrophysique de Paris, UMR7095 CNRS, Université Pierre & Marie Curie, 98bis boulevard Arago, 75014 Paris, France
[4] Observatoire de Haute-Provence, 04870 St-Michel L'Observatoire, France
[5] Laboratoire d'Astrophysique de Marseille, OAMP, Université Aix-Marseille and CNRS, 38 rue Frédéric Jolliot-Curie,
    13388 Marseille Cedex 13, France
[6] Physikalisches Institut Universität Bern, Sidlerstrasse 5, 3012 Bern, Switzerland
[7] Centro de Astrofísica, Universidade do Porto, Rua das Estrelas, 4150-762 Porto, Portugal
[8] Laboratoire d'Astrophysique de Grenoble, UMR5571 CNRS, Université Joseph Fourrier, BP 53, 38041 Grenoble Cedex 9, France
[9] Max-Planck-Institut für Astronomie, Königstuhl 17, 69117 Heidelberg, Germany

ABSTRACT

In this paper, we present our HARPS radial-velocity data for eight low-activity solar-type stars belonging to the HARPS volume-limited sample: HD 6718, HD 8535, HD 28254, HD 290327, HD 43197, HD 44219, HD 148156, and HD 156411. Keplerian fits to these data reveal the presence of low-mass companions around these targets. With minimum masses ranging from 0.58 to 2.54 $M_{\rm Jup}$, these companions are in the planetary mass domain. The orbital periods of these planets range from slightly less than one to almost seven years. The eight orbits presented in this paper exhibit a wide variety of eccentricities: from 0.08 to above 0.8.

Key words. planetary systems – techniques: radial velocities – techniques: spectroscopic

1. Introduction

In this paper, we present new detections from the HARPS planet search programme. It has been ongoing since 2003. Its detections are based on radial velocities obtained with the *High Accuracy Radial velocity Planet Searcher* (HARPS, Mayor et al. 2003). HARPS is a high-resolution echelle spectrograph mounted on the ESO–3.6-m telescope in La Silla (Chile). The instrument is installed in a vacuum vessel, and it is thermally controlled. These characteristics result in a very high stability of the intrumental radial-velocity zero point (measured drifts smaller than $1 \, {\rm m \, s^{-1}}$ over one night). HARPS possesses two optical fibres. The first one collects the target light, whereas the second one can be used for recording a reference Thorium-Argon spectrum. The second spectrum has been used for measuring the residual drift of the instrument since the time of the latest wavelength calibration, allowing us to apply a correction to the velocities (Baranne et al. 1996). The second fibre can also be used for measuring the spectrum of the sky background. With more than 70 detections

obtained so far, including the lightest planet (Gl 581 e, Mayor et al. 2009), the HARPS contribution to the exoplanet research field is a major one.

Since its beginning, the HARPS planet search programme has been divided into several sub-programmes related to specific scientific questions. One of these sub-programmes is the *HARPS volume-limited programme* to which about 20% of the HARPS Guaranteed Time Observation (GTO) programme allocated time was dedicated. The sample of the HARPS volume-limited programme is an extension up to 57.5 pc of the CORALIE planet search sample (volume-limited sample up to 50 pc, see Udry et al. 2000). It contains about 850 F8–M0 dwarfs. As in the case of the CORALIE sample, the maximum distance decreases with the $B - V$ colour index for targets with late spectral types (later than K0). Our target list will be published in another paper (Lo Curto et al., in prep.).

Targets in this sample are observed at lower signal-to-noise ratios (typically 40−50) than the ones in the high-precision programme and without using the simultaneous calibration. The typical photon-noise error obtained in this case is about $1−2 \, {\rm m \, s^{-1}}$ depending on the target spectral type and projected rotational velocity. This strategy, optimized for the follow-up of a large stellar sample, is a good compromise between precision and observing efficiency.

Rather short exposure times (less than 5 min) are usually enough for reaching the targeted signal-to-noise ratio. An

---

exposure time of 5 min is too short for correctly averaging out intrinsic stellar signals due for example to pulsation or granulation. Our velocities can thus be affected by those effects that in some cases can reach a peak-to-peak amplitude of several m s^{-1} (see e.g. the case of μ Arae, Santos et al. 2004a; Bouchy et al. 2005). The amplitudes of these signals depend on the target spectral types and on the averaging strategy. Expected radial-velocity errors due to intrinsic signals are greater for earlier spectral types and for evolved targets.

With such an observing strategy, our programme is mostly sensitive to Saturn or Jupiter-like planets but is also sensitive to lower-mass planets around stars with a low intrinsic radial-velocity variability. Also, we generally avoid taking exposures shorter than 1 min in order to reduce the impact of observing overheads. As a consequence, the brightest targets in our sample frequently have photon-noise errors significantly lower than the targetted one. For illustrating these facts, we mention the recent detections of a 5.5 $M_\oplus$ planet around HD 215497 (Lo Curto et al. 2010), of the 12.6 $M_\oplus$ planet HD 125595 b (Ségransan et al. 2010) and of the 14.4 $M_\oplus$ planet around BD −08 2823 b (Hébrard et al. 2010).

The main aim of this observational effort is a better characterization of orbital elements distributions of gaseous planets. With the increasing size of the sample of known planets, a quantitative comparison between the observed sample and the predictions of planet formation models becomes possible and reliable (see for example Mordasini et al. 2009). With the eight planetary companions presented in this paper, the total number of planets detected in the volume-limited sample now reaches 39 (see Pepe et al. 2004a; Moutou et al. 2005, 2009b; Lo Curto et al. 2006, 2010; Naef et al. 2007; Mordasini et al. 2010; Ségransan et al. 2010).

In this paper, we present our HARPS radial-velocity data for 8 solar-type stars hosting low-mass companions: HD 6718, HD 8535, HD 28254, HD 290327, HD 43197, HD 44219, HD 148156, and HD 156411. This paper is organized as follows. We present the main characteristics of the 8 host stars in Sect. 2. Section 3 contains the description of the radial-velocity sets and orbital solutions obtained for these targets. Finally, we provide concluding remarks in Sect. 4.

2. Characteristics of the host stars

We list the main characteristics of the nine host stars in Table 1. Apparent V-band magnitudes m_V and colour indexes $B - V$ are from the HIPPARCOS Catalogue (ESA 1997). Distances d are based on the improved HIPPARCOS astrometric parallaxes π derived by van Leeuwen (2007). Absolute magnitudes M_V were computed using m_V and d.

For each star, we derived the atmospheric parameters $T_{\rm eff}$, $\log g$, and [Fe/H] by performing a detailed local thermodynamical equilibrium spectroscopic analysis. A high signal-to-noise co-added HARPS spectrum was built for each target. The set of Fe I/Fe II equivalent widths used for the analysis were measured on the co-added spectra with the ARES code (Sousa et al. 2007). The list of spectral lines for the analysis, as well as more details on the method can be found in Santos et al. (2004b).

Stellar luminosities L were computed using HIPPARCOS apparent magnitudes and parallaxes and the bolometric correction obtained via the $T_{\rm eff}$-based calibration in Flower (1996). Stellar masses M_*, and radii R_* were derived from $T_{\rm eff}$, [Fe/H], and M_V by interpolating the Girardi et al. (2000) theoretical isochrones. Following Fernandes & Santos (2004), a relative

uncertainty of $\simeq$10% can be assumed for M_*. We also computed surface gravities, $\log g$, using M_* and R_*. These values are in fair agreement with the spectroscopic ones: a mean difference (spectroscopy−isochrones) of 0.06 dex and an rms of the differences equal to 0.11 dex. Spectral types listed in Table 1 are based on the stellar parameters we determined in this paper. Jenkins et al. (2008) have published iron abundances for HD 43197 and HD 148156. Their values, [Fe/H] = 0.37 ± 0.09 and 0.22 ± 0.15, respectively, are in good agreement with ours. The atmospheric parameters for HD 44219 have also been determined by Robinson et al. (2007). They found $T_{\rm eff}$ = 5723 ± 82, $\log g$ = 4.37 ± 0.13 and [Fe/H] = −0.05 ± 0.07. These values agree with ours within uncertainties.

Activity indexes $\log R'_{\rm HK}$ were extracted from individual HARPS spectra using a method similar to the one described in Santos et al. (2000). Values indicated in Table 1 are average activity indexes obtained for each target. All the targets exhibit a very low level of activity. Our $\log R'_{\rm HK}$ values for HD 43197 and HD 148156 are in good agreement with those published in Jenkins et al. (2008): −5.12 and −5.08, respectively. We did not try to estimate chromospheric ages for our targets because these two quantities are no longer correlated for weakly active stars (Pace & Pasquini 2004). However, we can infer for most of these stars (if not all) a safe age constraint based on their low activity indexes and rather high luminosities: age > 3 Gyr. The projected rotational velocities $v \sin i$ were derived from the widths of the HARPS cross-correlation functions (CCF) following the method presented in Santos et al. (2002).

Finally, HD 28254 is the bright component of a visual binary. According to the Catalogue of Components of Double and Multiple stars (Dommanget & Nys 2002), the visual companion, CCDM J04248-5037 B, is located at a separation of 4.3″ and at a position angle of 254 degrees. With an apparent magnitude of m_V = 13.8, this object is 6.11 mag fainter (i.e. a flux ratio less than 0.4%). It was thus clearly outside the detection capabilities of HIPPARCOS. Assuming the two stars form a bound system and using the distance of HD 28254 (54.7 pc), we computed the projected separation between them: 235 AU. We also computed the absolute magnitude of the B component: M_V = 10.11 corresponding to an M0V-M2V star. With this absolute magnitiude and the mass-luminosity relations in Delfosse et al. (2000), we computed a mass of 0.48 $M_\odot$ for this object. Its minimum period is about 1000 yr. Assuming that this companion is on a circular edge-on orbit, the maximal radial-velocity amplitude it would induce on the primary star is of the order of 1.1 km s^{-1}.

3. HARPS radial-velocity data and orbital solutions

As explained before, stars belonging to the HARPS volume-limited sample are generally observed without simultaneous thorium-argon reference. Possible instrumental drifts therefore remain uncorrected. This has only a limited impact on our results because: 1) the instrument is very stable: on average, the radial-velocity drifts of HARPS remain below 0.5 m s^{-1} over one night and 2) the targetted photon-noise error for this programme is 1−2 m s^{-1}. We stress again the fact that our observing strategy is not optimally designed for averaging out stellar intrinsic signals. We list in Table 2 the median exposure times for all the targets. This median is below 3 min in all cases. We thus expect our velocities to be affected at some level by stellar intrinsic jitter in particular the velocities of our early type and/or slightly evolved targets, namely HD 8535 (G0V), HD 28254 (G1IV/V), HD 148156 (F8V), and HD 156411 (F8IV/V).

Table 1. Observed and inferred stellar characteristics of the host stars.

Parameter	Unit	HD 6718	HD 8535	HD 28254	HD 290327
Sp. Type		G5V	G0V	G1IV/V	G8V
m_V		8.45	7.70	7.69	8.99
$B - V$		0.662	0.553	0.722	0.761
π	(mas)	18.23 ± 0.76	19.03 ± 0.60	18.29 ± 0.53	17.65 ± 1.57
d	(pc)	$54.9^{+2.4}_{-2.2}$	$52.5^{+1.7}_{-1.6}$	$54.7^{+1.6}_{-1.5}$	$56.7^{+5.5}_{-4.6}$
M_V		4.754	4.097	4.001	5.224
B.C.		-0.145	-0.028	-0.102	-0.126
L	$(L_\odot)$	1.13	1.86	2.18	0.72
$T_{\rm eff}$	(K)	5746 ± 19	6136 ± 18	5664 ± 35	5552 ± 21
$\log g^a$	(cgs)	4.48 ± 0.03	4.46 ± 0.06	4.12 ± 0.05	4.42 ± 0.04
$\log g^b$	(cgs)	4.40	4.35	4.13	4.39
[Fe/H]		-0.06 ± 0.02	0.06 ± 0.02	0.36 ± 0.03	-0.11 ± 0.02
M_*	$(M_\odot)$	0.96	1.13	1.06	0.90
R_*	$(R_\odot)$	1.02 ± 0.03	1.19 ± 0.04	1.48 ± 0.06	1.00 ± 0.01
$\log R'_{HK}$		-4.97	-4.95	-5.10	-4.96
$v \sin i$	$(\mathrm{km\,s^{-1}})$	1.76 ± 1.0	1.41 ± 1.0	2.50 ± 1.0	1.44 ± 1.0
Parameter	Unit	HD 43197	HD 44219	HD 148156	HD 156411
Sp. Type		G8V	G2V	F8V	F8IV/V
m_V		8.98	7.69	7.69	6.67
$B - V$		0.817	0.687	0.560	0.614
π	(mas)	17.76 ± 1.22	19.83 ± 0.78	19.38 ± 0.75	18.25 ± 0.49
d	(pc)	$56.3^{+4.2}_{-3.6}$	$50.4^{+2.1}_{-1.9}$	$51.6^{+2.1}_{-1.9}$	$54.8^{+1.5}_{-1.4}$
M_V		5.227	4.177	4.127	2.976
B.C.		-0.137	-0.085	-0.009	-0.060
L	$(L_\odot)$	0.73	1.82	1.78	5.38
$T_{\rm eff}$	(K)	5508 ± 46	5752 ± 16	6308 ± 28	5900 ± 15
$\log g^a$	(cgs)	4.31 ± 0.08	4.21 ± 0.03	4.56 ± 0.07	4.07 ± 0.04
$\log g^b$	(cgs)	4.42	4.20	4.36	3.87
[Fe/H]		0.40 ± 0.04	0.03 ± 0.01	0.29 ± 0.02	-0.12 ± 0.01
M_*	$(M_\odot)$	0.96	1.00	1.22	1.25
R_*	$(R_\odot)$	1.00 ± 0.01	1.32 ± 0.07	1.21 ± 0.03	2.16 ± 0.09
$\log R'_{HK}$		-5.06	-5.03	-4.94	-5.05
$v \sin i$	$(\mathrm{km\,s^{-1}})$	2.18 ± 1.0	2.22 ± 1.0	5.70 ± 1.0	3.30 ± 1.0

Notes. [a] From our spectroscopic LTE analysis; [b] using M_* and R_*.

Our radial velocities can be obtained from the extracted spectra by cross-correlating them with a numerical template. Numerical templates are chosen to minimize the mismatch with the target spectral type. Our radial-velocity uncertainties include two well-quantified contributions: photon noise and calibration error. An additional error of $0.5\,\mathrm{m\,s^{-1}}$ is added quadratically to account for the absence of simultaneous calibration and thus the possibility of a small uncorrected radial-velocity drift of the HARPS zero point.

All the orbital solutions presented in the following sections were obtained with software that includes a genetic algorithm. In general, the only a priori information used by this algorithm is the type of model we want to use (i.e., 1-Keplerian, 2-Keplerian, 1-Keplerian plus a linear/quadratic drift, etc.). Once the global parameter space minimum is identified, we use it as the starting point for a standard Levenberg-Marquardt minimization out of which the final solution is obtained. In all the cases, we have verified the absence of correlation between the post-fit residuals and the measured cross-correlation function bisectors.

Finally, uncertainities on the fitted parameters are determined using Monte-Carlo simulations.

3.1. HD 6718

The 22 HARPS radial-velocity measurements were gathered for HD 6718 (HIP 5301) between BJD = 2 452 991 (December 18, 2003) and BJD = 2 455 019 (July 6, 2009). These velocities have a mean uncertainty of $1.59\,\mathrm{m\,s^{-1}}$. We have fitted a long-period Keplerian orbit to these data. The orbital parameters resulting from this fit are listed in Table 2. With these parameters and assuming a mass of $0.96\,M_\odot$ for the host star, we computed a minimum mass of $1.56\,M_{\rm Jup}$ for the companion and a semi-major axis of 3.56 AU. Residuals to the fitted orbit have a very low dispersion ($\sigma_{\rm O-C} = 1.79\,\mathrm{m\,s^{-1}}$), and a 1-planet model is thus sufficient for explaining the detected signal. We display our data and the fitted orbit in panel **a** of Fig. 1.

Table 2. Orbital solutions for the eight host stars.

Parameter	Unit	HD 6718	HD 8535	HD 28254	HD 290327
P	(d)	2496 ± 176	1313 ± 28	1116 ± 26	2443^{+205}_{-117}
T	(JD[a])	357 ± 251	537 ± 92	49^{+43}_{-55}	1326^{+230}_{-412}
e		$0.10^{+0.11}_{-0.04}$	$0.15^{+0.09}_{-0.05}$	$0.81^{+0.05}_{-0.02}$	$0.08^{+0.08}_{-0.03}$
γ	(km s^{-1})	34.7509 ± 0.0013	2.4588 ± 0.0008	$-9.315^{b} \pm 0.002$	29.559 ± 0.003
ω	(deg)	286^{+64}_{-35}	61^{+18}_{-43}	301^{+3}_{-4}	268^{+94}_{-19}
K_1	(m s^{-1})	24.1 ± 1.5	11.8 ± 0.8	$37.3^{+5.1}_{-0.9}$	41.3 ± 2.9
Slope	(m s^{-1} yr^{-1})	...	...	2.629 ± 0.015	...
Curvature	(m s^{-1} yr^{-2})	...	...	-0.9290 ± 0.00012	...
$f(m)$	($10^{-9} M_\odot$)	$3.56^{+0.71}_{-0.52}$	$0.22^{+0.06}_{-0.04}$	$1.22^{+0.30}_{-0.17}$	$17.6^{+3.2}_{-2.3}$
$a_1 \sin i$	(10^{-3} AU)	$5.50^{+0.45}_{-0.24}$	$1.41^{+0.11}_{-0.09}$	$2.25^{+0.19}_{-0.13}$	$9.24^{+0.61}_{-0.29}$
$m_2 \sin i$	($M_{\rm Jup}$)	$1.56^{+0.11}_{-0.10}$	$0.68^{+0.07}_{-0.04}$	$1.16^{+0.10}_{-0.06}$	$2.54^{+0.17}_{-0.14}$
a	(AU)	$3.56^{+0.24}_{-0.15}$	$2.45^{+0.04}_{-0.06}$	$2.15^{+0.04}_{-0.05}$	$3.43^{+0.20}_{-0.12}$
$N_{\rm mes}$		22	45	32	18
Med($t_{\rm exp}$)	(s)	158	106	60	173
$\langle S/N \rangle$		52	58	51	45
$\langle \epsilon_{\rm RV} \rangle$	(m s^{-1})	1.59	1.57	1.34	1.73
Span	(d)	2028	2220	1989	1986
$\sigma_{\rm O-C}$	(m s^{-1})	1.79	2.49	2.19	1.60
$\chi^2_{\rm red}$		1.50	2.48	3.08	1.22
Parameter	**Unit**	**HD 43197**	**HD 44219**	**HD 148156**	**HD 156411**
P	(d)	327.8 ± 1.2	$472.3^{+6.3}_{-5.0}$	1027 ± 28	842.2 ± 14.5
T	(JD[a])	713.8 ± 1.7	$585.6^{+7.2}_{-3.1}$	707 ± 20	356^{+46}_{-33}
e		$0.83^{+0.05}_{-0.01}$	$0.61^{+0.07}_{-0.09}$	$0.52^{+0.04}_{-0.09}$	0.22 ± 0.08
γ	(km s^{-1})	72.512^{+4}_{-11}	$-12.0732^{c} \pm 0.0026$	$-1.7480^{+0.0013}_{-0.0009}$	-38.7512 ± 0.0011
ω	(deg)	251^{+7}_{-12}	$147.4^{+6.2}_{-3.2}$	35^{+17}_{-12}	45^{+22}_{-14}
K_1	(m s^{-1})	$32.4^{+10.9}_{-3.3}$	19.4 ± 3.0	$17.5^{+1.5}_{-0.5}$	14.0 ± 0.8
Slope	(m s^{-1} yr^{-1})	...	-0.637 ± 0.016	...	...
Curvature	(m s^{-1} yr^{-2})	...	-0.76390 ± 0.000	...	...
$f(m)$	($10^{-9} M_\odot$)	$0.21^{+0.13}_{-0.04}$	$0.17^{+0.05}_{-0.03}$	$0.35^{+0.08}_{-0.04}$	$0.23^{+0.04}_{-0.03}$
$a_1 \sin i$	(10^{-3} AU)	$0.55^{+0.10}_{-0.04}$	$0.66^{+0.06}_{-0.04}$	$1.41^{+0.09}_{-0.06}$	$1.06^{+0.08}_{-0.05}$
$m_2 \sin i$	($M_{\rm Jup}$)	$0.60^{+0.12}_{-0.04}$	$0.58^{+0.06}_{-0.04}$	$0.85^{+0.06}_{-0.05}$	$0.74^{+0.05}_{-0.04}$
a	(AU)	$0.92^{+0.01}_{-0.02}$	1.19 ± 0.02	$2.45^{+0.04}_{-0.05}$	$1.88^{+0.03}_{-0.04}$
$N_{\rm mes}$		33	46	42	50
Med($t_{\rm exp}$)	(s)	171	63	92	90
$\langle S/N \rangle$		48	51	56	73
$\langle \epsilon_{\rm RV} \rangle$	(m s^{-1})	1.42	1.55	2.24	1.26
Span	(d)	1943	1988	2168	2231
$\sigma_{\rm O-C}$	(m s^{-1})	1.44	2.39	3.69	2.94
$\chi^2_{\rm red}$		1.19	2.62	2.89	5.21

Notes. Errobars are Monte-Carlo based 1σ uncertainties. $\langle \epsilon_{\rm RV} \rangle$ is the radial-velocity uncertainty weighted average. $\sigma_{\rm O-C}$ is the weighted rms of the residuals to the fitted orbits. Med($t_{\rm exp}$) is the median exposure time and $\langle S/N \rangle$ is the average signal-to-noise ratio at 550 nm. [a] JD = BJD$-2\,454\,000$; [b] at BJD $=2\,454\,106.6$; [c] at BJD $=2\,454\,512.6$.

3.2. HD 8535

A set of 45 HARPS radial velocities was obtained for HD 8535 (HIP 6511) between BJD $= 2\,452\,850$ (July 29, 2003) and BJD $= 2\,455\,070$ (August 26, 2009). The mean radial-velocity uncertainty of these measurements is 1.57 m s^{-1}. The presence of a long-period signal is obvious (see panel **b** of Fig. 1). The results of the Keplerian fit to our data are presented in Table 2. The

dispersion of the residuals to the fitted orbit are somewhat larger than expected ($\chi^2_{\rm red} = 2.48$). We have tried to fit orbits including additional signals (linear or quadratic trend; 2-Keplerian model) but we were unable to significantly improve the quality of the solution. We have also verified the absence of any correlation between the residuals and the CCF bisectors.

Assuming a primary mass of $1.13 M_\odot$, we computed the minimum mass of the companion and the semi-major axis of its
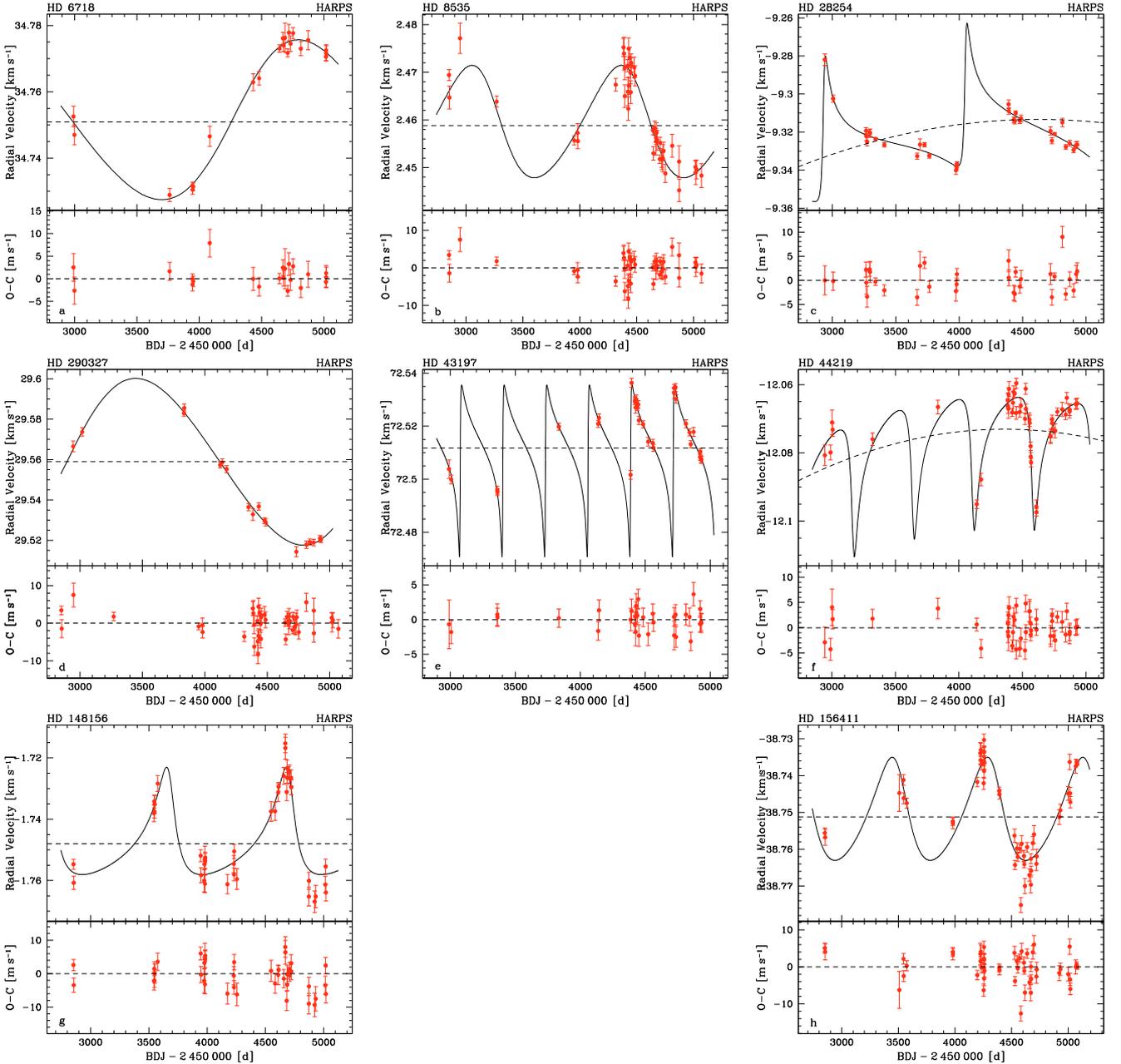
Fig. 1. HARPS radial-velocity data for the eight stars presented in this paper. Temporal velocities (filled dots) and fitted orbital solutions (solid lines) are displayed in *the upper panels*. Residuals to the fitted orbits are displayed in *the bottom panels*. For HD 28254 and HD 44219, the dashed lines in the upper panels show additional quadratic radial-velocity drifts that were included to the orbital fits. For all the other targets, the *upper panels* dashed lines represent the systemic velocity γ.

orbit: $m_2 \sin i = 0.68\,M_{\rm Jup}$ and $a = 2.45$ AU. The fitted orbit and the fit residuals are displayed in panel **b** of Fig. 1. The phase-folded orbit and velocities are displayed in panel **a** of Fig. 2.

3.3. HD 28254

We collected 32 HARPS radial velocities for HD 28254 (HIP 20606) between BJD = 2 452 941 (October 28, 2003) and BJD = 2 454 931 (April 9, 2009). The average velocity uncertainty of these measurements is $1.34\,{\rm m\,s^{-1}}$. As indicated in Sect. 2, HD 28254 is the main component of a visual binary system. The presence of a nearby visual companion can induce radial-velocity errors via the seeing-dependent contamination of the spectrum of the main component. Pepe et al. (2004b) have

simulated this effect for HARPS and using the La Silla seeing statistics. We have performed the same simulations using the characteristics of the HD 28254 system ($\rho = 4.3''$, $\Delta m_V = 6.11$). The expected effect is negligible in this case ($\ll 0.1\,{\rm m\,s^{-1}}$).

A long-period signal is visible on the data (see panel **c** of Fig. 1). From the visual inspection of these data, it is also obvious that the Keplerian signal is highly eccentric. We first attempted to fit a single orbit to our velocities. With $e > 0.99$, the obtained orbit was not physical so we rejected it. After this initial unsuccessful attempt, we tried to fit orbits with additional signals. The following two models did not give satisfactory results: the 1-Keplerian plus linear drift model and the 2-Keplerian one. The best fit we obtained and finally adopted is based on a 1-Keplerian plus quadratic drift model. Despite the
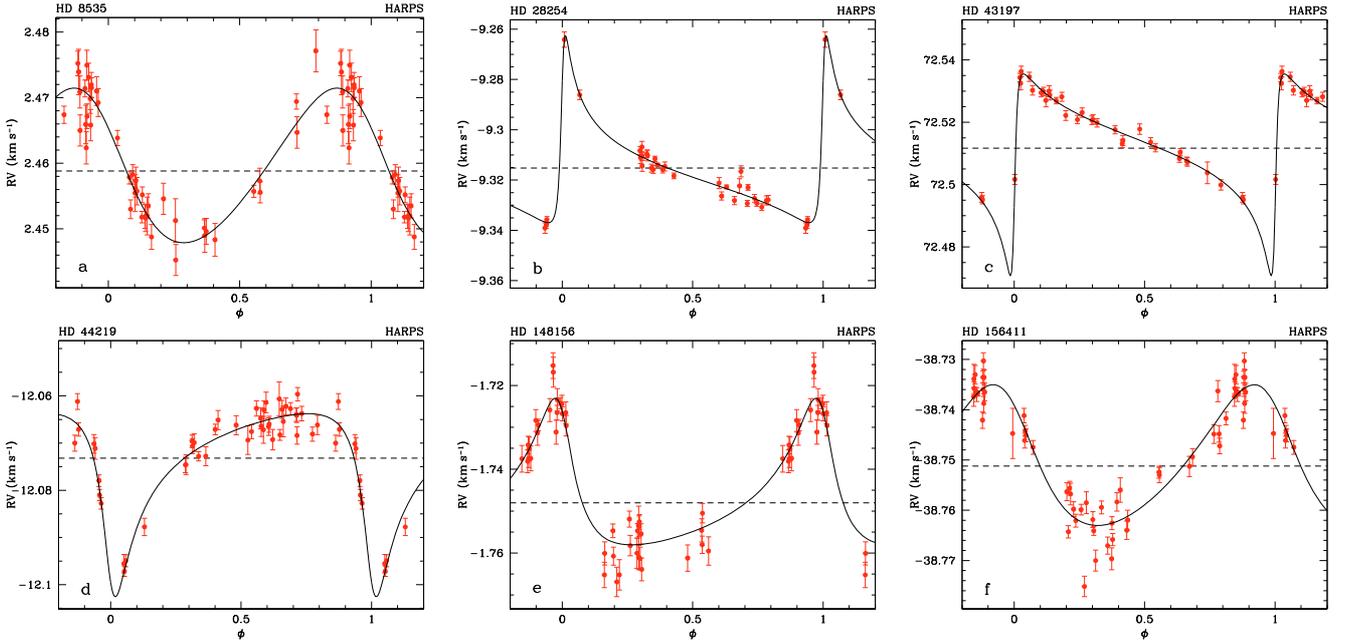
Fig. 2. HARPS phase-folded velocities and fitted orbits for the 6 targets observed for at least two orbital periods. The radial-velocities of HD 28254 and HD 44219 have been corrected for the fitted quadratic drift.

poor coverage of the second radial-velocity maximum, hence the poorly constrained velocity semi-amplitude, the planetary nature of HD 23254 b is well established. The orbital period is very well constrained. Solutions with significantly larger amplitudes are possible, but they also have much larger eccentricities. The effect of the increasing amplitude on the minimum mass of the companion is largely compensated for by the increasing eccentricity as the mass function scales with $K_1^3(1 - e^2)^{3/2}$.

More data are necessary for better constraining the shape of the orbit of HD 28254 b. In particular, a better coverage of the periastron passage will allow us to constrain the radial-velocity semi-amplitude and orbital eccentricity. These future observations will also help us characterizing the secondary signal better. The orbital solution we present here is thus a preliminary one. The observed additional quadratic signal remains compatible with the signal that the visual companion described in Sect. 2 could induce.

Using our fitted parameters, we computed the minimum mass of the planetary companion and its orbital semi-major axis: $m_2 \sin i = 1.16 \, M_{\rm Jup}$ and $a = 2.15$ AU. Our radial-velocity data and the fitted orbit are displayed in panel **c** of Fig. 1. The phase-folded orbit and velocities are displayed in panel **b** of Fig. 2.

3.4. HD 290327

Between BJD = 2 452 945 (November 1, 2003) and BJD = 2 454 931 (April 9, 2009), we have observed HD 290327 (HIP 25191) 18 times with HARPS. The obtained radial velocities have a mean uncertainty of $1.73 \, \mathrm{m\,s^{-1}}$. A long-period signal is well visible on the data. We list in Table 2 the parameters resulting from a Keplerian fit to the data. With these parameters and using the primary mass of Table 1 (0.90 $M_\odot$), we computed the minimum mass of the companion that induces the detected radial-velocity signal and the semi-major axis of its orbit: $m_2 \sin i = 2.54 \, M_{\rm Jup}$ and $a = 3.43$ AU. The dispersion of the residuals to the fitted orbit is very low: $1.6 \, \mathrm{m\,s^{-1}}$. Our velocity data and the fitted orbit are displayed in panel **d** of Fig. 1.

3.5. HD 43197

We have gathered a set of 33 radial velocities for HD 43197 (HIP 29550). These data were obtained between BJD = 2 452 989 (December 15, 2003) and BJD = 2 454 932 (April 10, 2009), and they have a mean velocity uncertainty of $1.42 \, \mathrm{m\,s^{-1}}$. A visual inspection of the data displayed in panel **e** of Fig. 1 shows a periodic highly eccentric signal. The parameters resulting from a Keplerian fit to the data are listed in Table 2. The fitted eccentricity is indeed very high and very well constrained in spite of our poor coverage of the radial-velocity minimum. The rms of the residuals to the fitted orbit is very low: $1.42 \, \mathrm{m\,s^{-1}}$. This 1-planet fit is thus satisfactory. With a primary mass of $0.96 \, M_\odot$, the computed minimum mass of the companion is $0.6 \, M_{\rm Jup}$. The orbital semi-major axis is 0.92 AU. Our data, the fitted orbit, and the residuals are displayed in panel **e** of Fig. 1. Panel **c** of Fig. 2 shows the phase-folded orbit.

3.6. HD 44219

The HARPS data set we have in hand for HD 44219 (HIP 30114) consists of 46 radial velocities measured between BJD = 2 452 944 (October 31, 2003) and BJD = 2 454 932 (April 10, 2009). These velocities have an average uncertainty of $1.55 \, \mathrm{m\,s^{-1}}$. We first fitted a 1-Keplerian model to these data. The residuals to this fitted orbit were a bit large ($\sigma_{\rm O-C} = 2.95 \, \mathrm{m\,s^{-1}}$). We then tried to include an additional signal in the fitted model. Adding a linear drift improved the quality of the fit in a marginally significant way ($\chi_{\rm red}^2$ decreasing from 3.79 to 3.30; f-test probability = 71%). The improvement resulting from including a quadratic trend in the fitted model was more significant: $\chi_{\rm red}^2 = 2.62$ and f-test probability equals 90%. We also tried to fit a 2-planet model but we were unable to find any convincing solution. We finally decided to adopt the Keplerian + quadratic drift model. The parameters resulting from this fit are listed in Table 2. The orbital parameters obtained with our initial 1-planet fit did not differ much from the ones in the adopted solution ($P = 447$ d; $e = 0.57$; $K_1 = 17 \, \mathrm{m\,s^{-1}}$ and $m_2 \sin i = 0.52 \, M_{\rm Jup}$).

The dispersion of the residuals to the finally selected solution is still a bit large ($\sigma_{O-C} = 2.39\,\mathrm{m\,s^{-1}}$), but this is probably due to the still not very well constrained additional signal. With this solution and assuming $M_* = 1\,M_\odot$, the computed minimum mass for HD 44219 b is $0.58\,M_{\mathrm{Jup}}$ and its orbital semi-major axis is 1.19 AU. We display the fitted model and the temporal residuals in panel **f** of Fig. 1. The phase-folded orbit and velocities are displayed in panel **d** of Fig. 2.

3.7. HD 148156

We have collected 42 radial velocities with HARPS for HD 148156 (HIP 80680) between BJD = 2 452 852 (July 31, 2003) and BJD = 2 455 020 (July 7, 2009). The mean radial-velocity uncertainty of this data set is $2.24\,\mathrm{m\,s^{-1}}$. A long-period signal is visible in the data displayed in panel **g** of Fig. 1. The results of the Keplerian fit performed on our velocity set are presented in Table 2. The rms of the residuals is a bit large ($\sigma_{O-C} = 3.69\,\mathrm{m\,s^{-1}}$; $\chi^2_{\mathrm{red}} = 2.89$). We were unable to significantly improve the fit by adding extra signals. No obvious correlation between CCF bisectors and residuals could be detected. The origin of these abnormal residuals remains unknown, but they may be due to intrinsic stellar jitter.

The minimum mass of HD 148156 b is $0.85\,M_{\mathrm{Jup}}$ and the semi-major axis of its orbit is 2.45 AU (assuming $M_* = 1.22\,M_\odot$). The fitted orbit and the fit residuals are displayed in panel **g** of Fig. 1. The phase-folded orbit and velocities are displayed in panel **e** of Fig. 2.

3.8. HD 156411

We obtained 50 HARPS radial-velocity measurements of HD 156411 (HIP 84787). These measurements were taken between BJD = 2 452 850 (July 29, 2003) and BJD = 2 455 081 (September 6, 2009) and they have a mean velocity uncertainty of $1.26\,\mathrm{m\,s^{-1}}$. A long-period signal is visible on the data displayed in panel **h** of Fig. 1. We fitted a Keplerian orbit to these data. The resulting parameters are listed in Table 2. The dispersion of the residuals to the fitted orbit is too large ($\sigma_{O-C} = 2.94\,\mathrm{m\,s^{-1}}$), and the fit quality quite poor ($\chi^2_{\mathrm{red}} = 5.21$).

We tried to fit models including additional signals. First, we tried to add linear and quadratic drifts. In both cases, the fit quality improved a bit ($\chi^2_{\mathrm{red}} = 4.80$ and 4.70, respectively) but the corresponding f-test probabilities indicated that the achieved improvements were only marginally significant (at the 1σ level). A 2-planet fit was also tried, but we were unable to find any convincing solution. We also verified the absence of correlation between CCF bisectors and residuals. HD 156411 is slightly evolved so we speculate that intrinsic stellar signals are responsible for the abnormal residuals.

For this paper, we finally decided to adopt our initial 1-planet orbital solution. With this solution and assuming a mass of $1.25\,M_\odot$ for the host star, we computed a minimum mass of $0.74\,M_{\mathrm{Jup}}$ and an orbital semi-major axis of 1.88 AU for HD 156411 b. The fitted orbit and the temporal residuals are displayed in panel **h** of Fig. 1. The phase-folded orbit and velocities are displayed in panel **f** of Fig. 2.

4. Conclusions

In this paper, we have presented our HARPS radial-velocity data for 8 low-activity solar-type stars orbited by at least one long-period planetary companion. HD 6718 has a $1.56\,M_{\mathrm{Jup}}$

companion on a 2496-d low-eccentricity orbit ($e = 0.1$). The companion orbiting HD 8535 is a $0.68\,M_{\mathrm{Jup}}$ planet with a period of 1313 days and an eccentricity of 0.15. HD 28254 b is a $1.16\,M_{\mathrm{Jup}}$ planet on a 1116-d highly eccentric orbit ($e = 0.81$). The companion to HD 290327 has a minimum mass of $2.54\,M_{\mathrm{Jup}}$. Its 2442-d orbit is nearly circular ($e = 0.08$). As for HD 28254 b, the $0.6\,M_{\mathrm{Jup}}$ companion to HD 43197 is on a highly eccentric orbit: $e = 0.83$. Its orbital period is 327 d. HD 44219 is orbited by a $0.58\,M_{\mathrm{Jup}}$ planet on a 472-d 0.61 eccentricity orbit. HD 148156 b is a $0.85\,M_{\mathrm{Jup}}$ planet orbiting its parent star on a 1027-d eccentric orbit ($e = 0.52$) and the companion to HD 156411 is a 0.74 Jupiter-mass planet with a mildly eccentric ($e = 0.22$) 842-d orbit.

We find some evidence of additional longer-period companions around HD 28254 and HD 44219. In both cases, we are unable to fit full double-Keplerian orbits because of our short observing time span. Future observations of these two systems will probably allow us to better characterize the companions responsible for these signals.

Finally, with the addition of HD 28254 b and HD 43197 b, the population of exoplanets with extremely high eccentricities now amounts to 6. The other planets with $e \geq 0.8$ are HD 4113 ($e = 0.903$, Tamuz et al. 2008), 156846 ($e = 0.8472$, Tamuz et al. 2008), HD 20782 b ($e = 0.92$, Jones et al. 2006), and HD 80606 b ($e = 0.934$, Moutou et al. 2009a). Five of these stars hosting highly eccentric planets are members of wide visual binaries (see Tamuz et al. 2008 for HD 4113 and HD 156846, Desidera & Barbieri 2007 for HD 20792, and Naef et al. 2001 for HD 80606). Only HD 43197 is not known to be in a multiple stellar system. This large number of eccentric-planet hosts in binaries tend to favour scenarios in which the extreme orbital eccentricity results from the influence of a third body via Kozai oscillations (Kozai 1962) or Kozai migration (Wu & Murray 2003).

References

Baranne, A., Queloz, D., Mayor, M., et al. 1996, A&AS, 119, 373
Bouchy, F., Bazot, M., Santos, N. C., Vauclair, S., & Sosnowska, D. 2005, A&A, 440, 609
Delfosse, X., Forveille, T., Ségransan, D., et al. 2000, A&A, 364, 217
Desidera, S., & Barbieri, M. 2007, A&A, 462, 345
Dommanget, J., & Nys, O. 2002, IAU Commission on Double Stars, 148, 4
ESA. 1997, The HIPPARCOS and TYCHO catalogue, ESA-SP, 1200
Fernandes, J., & Santos, N. C. 2004, A&A, 427, 607
Flower, P. J. 1996, ApJ, 469, 355
Girardi, L., Bressan, A., Bertelli, G., & Chiosi, C. 2000, A&AS, 141, 371
Hébrard, G., Udry, S., Lo Curto, G., et al. 2010, A&A, 512, A46
Jenkins, J. S., Jones, H. R. A., Pavlenko, Y., et al. 2008, A&A, 485, 571
Jones, H. R. A., Butler, R. P., Tinney, C. G., et al. 2006, MNRAS, 369, 249
Kozai, Y. 1962, AJ, 67, 591
Lo Curto, G., Mayor, M., Clausen, J. V., et al. 2006, A&A, 451, 345
Lo Curto, G., Mayor, M., Benz, W., et al. 2010, A&A, 512, A48
Mayor, M., Bonfils, X., Forveille, T., et al. 2009, A&A, 507, 487
Mayor, M., Pepe, F., Queloz, D., et al. 2003, The Messenger, 114, 20
Mordasini, C., Alibert, Y., Benz, W., & Naef, D. 2009, A&A, 501, 1161
Mordasini, C., Mayor, M., Udry, S., et al. 2010, A&A, accepted
Moutou, C., Mayor, M., Bouchy, F., et al. 2005, A&A, 439, 367
Moutou, C., Hébrard, G., Bouchy, F., et al. 2009a, A&A, 498, L5

Moutou, C., Mayor, M., Lo Curto, G., et al. 2009b, A&A, 496, 513
Moutou, C., Mayor, M., Lo Curto, G., et al. 2010, A&A, submitted
Naef, D., Latham, D. W., Mayor, M., et al. 2001, A&A, 375, L27
Naef, D., Mayor, M., Benz, W., et al. 2007, A&A, 470, 721
Pace, G., & Pasquini, L. 2004, A&A, 426, 1021
Pepe, F., Mayor, M., Queloz, D., et al. 2004a, A&A, 423, 385
Pepe, F., Mayor, M., Queloz, D., & Udry, S. 2004b, in Planetary Systems in the Universe, ed. A. Penny, IAU Symp., 202, 103
Robinson, S. E., Ammons, S. M., Kretke, K. A., et al. 2007, ApJS, 169, 430
Santos, N. C., Mayor, M., Naef, D., et al. 2000, A&A, 361, 265
Santos, N. C., Mayor, M., Naef, D., et al. 2002, A&A, 392, 215
Santos, N. C., Bouchy, F., Mayor, M., et al. 2004a, A&A, 426, L19
Santos, N. C., Israelian, G., & Mayor, M. 2004b, A&A, 415, 1153
Ségransan, D., Mayor, M., Udry, S., et al. 2010, A&A, submitted
Sousa, S. G., Santos, N. C., Israelian, G., Mayor, M., & Monteiro, M. J. P. F. G. 2007, A&A, 469, 783
Tamuz, O., Ségransan, D., Udry, S., et al. 2008, A&A, 480, L33
Udry, S., Mayor, M., Queloz, D., Naef, D., & Santos, N. 2000, in From Extrasolar Planets to Cosmology: The VLT Opening Symposium, ed. J. Bergeron, & A. Renzini, 571
van Leeuwen, F. 2007, A&A, 474, 653
Wu, Y., & Murray, N. 2003, ApJ, 589, 605